

# MOFO: MOTion FOCused Self-Supervision for Video Understanding

Mona Ahmadian  
m.ahmadian@surrey.ac.uk

Frank Guerin  
f.guerin@surrey.ac.uk

Andrew Gilbert  
a.gilbert@surrey.ac.uk

University of Surrey  
Guildford, UK

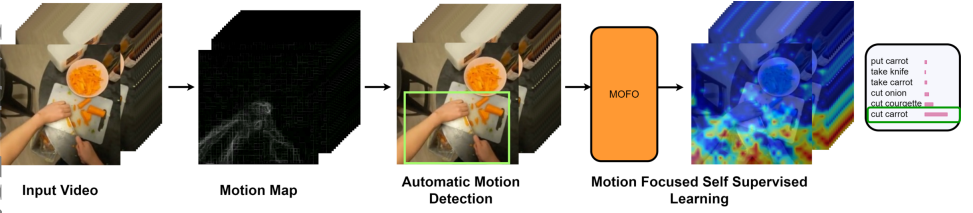


Figure 1: MOFO is a motion focused self supervised framework for egocentric action recognition.

## Abstract

Self-supervised learning (SSL) techniques have recently produced outstanding results in learning visual representations from unlabeled videos. Despite the importance of motion in supervised learning techniques for action recognition, SSL methods often do not explicitly consider motion information in videos. To address this issue, we propose MOFO (MOTion FOCused), a novel SSL method for focusing representation learning on the motion area of a video, for action recognition. MOFO automatically detects motion areas in videos and uses these to guide the self-supervision task. We use a masked auto-encoder which randomly masks out a high proportion of the input sequence; we force a specified percentage of the inside of the motion area to be masked and the remainder from outside. We further incorporate motion information into the finetuning step to emphasise motion in the downstream task. We demonstrate that our motion-focused innovations can significantly boost the performance of the currently leading SSL method (VideoMAE) for action recognition. Our method improves the recent self-supervised Vision Transformer (ViT), VideoMAE, by achieving +2.6%, +2.1%, +1.3% accuracy on Epic-Kitchens verb, noun and action classification, respectively, and +4.7% accuracy on Something-Something V2 action classification. Our proposed approach significantly improves the performance of the current SSL method for action recognition, indicating the importance of explicitly encoding motion in SSL. To enable the reproduction and improvement of our work, the code is available<sup>1</sup>.

# 1 Introduction

Action recognition is an essential task in video understanding and has been extensively investigated in recent years [16, 26, 40]. In video action recognition, supervised deep learning techniques have made significant progress [13, 25, 32]; However, due to the lack of labels, which must be manually collected, learning to recognise actions from a small number of labelled videos is a difficult task as data collection will be expensive and challenging. It is especially inappropriate for long-tail open vocabulary object distributions across scenes, such as a kitchen. Furthermore, getting annotations for videos is much more difficult due to the large number of frames and the temporal boundaries of when actions begin and end. Therefore SSL has gained attention due to the problems above. In SSL, a model is trained using data and labels, but in this case, the labels come from the data itself without expensive and limiting human annotation.

Supervised methods [39] have recognised the importance of motion to understanding actions because often, key objects are moving in the scene. However, most SSL methods do not explicitly consider motion or use hand-crafted features [10], limiting their effectiveness. While for SSL, masked autoencoder models [33] have been proposed to learn underlying data distribution in a self-supervised manner without explicitly focusing on the motion. Even though this model can perform spatiotemporal reasoning over content, the encoder backbone is ineffective in capturing motion representations (we show this later in Fig. 4). While other works encode long/short-term interdependence [22, 29] and temporal pooling [42], these works rely on human-annotated labels or supervised models to extract motion. Thus, large-scale annotations are typically not feasible. Incorporating motion information is not trivial, though, as one of the significant downsides of using optical flow features to detect motion, especially in egocentric video, is the stability of the results, as it will be affected by camera motion, with static objects or background pixels exhibiting high movement velocities in optical flow when the camera moves rapidly.

Therefore we propose to detect salient objects and motion in the video without the overhead and limitation of a pretrained and annotated object detector. This automatic approach for object detection is based on motion boundaries from optical flow. Using the motion boundaries instead of a direct optical flow output mitigates the challenge of camera motion and creates salient areas of movement or interest without a pretrained network. To fully exploit this phenomenon, in this work, we propose a motion-aware self-supervised approach, **MOFO**, to perform self-supervised video action recognition. The key contribution is explicitly imposing motion information in both SSL phases in the self-supervised pretext training without human annotations and then in the finetuning stage. Given the identification of motion, we propose to provide a motion understanding of the now familiar self-supervised masking [33] of small regions or 3D patches in the video frames. Then during the finetuning stage, MOFO prioritises the motion areas in video data identified as a self-supervision pretext task. Since motion areas contain more information, such as moving objects, actions, and interactions, our proposed model gives them a higher priority by emphasising the masking strategy to be more in the motion area.

In summary, MOFO’s contributions are as follows:

- The Automatic motion area detection using motion maps driven by optical flows, but invariant to camera motion.
- A motion-aware SSL approach, which focuses masking on the motion area in the video, using our proposed automatic motion detection algorithm.

- A motion-focused finetuning technique to further intensify the focus on the motion area for the action recognition task.
- The demonstration of our model’s state-of-the-art performance for SSL action recognition on two large benchmark datasets *Epic-Kitchens* and *Something Something V2*.

## 2 Related Work

**Self-supervised Learning in Video:** SSL has gained considerable popularity since its introduction in natural language processing [8] and computer vision [5, 9, 40] owing to its ability to learn effective data representations without requiring manual labels. Acquiring detailed manual labels is arguably more difficult (and often expensive) in many image and video related tasks, which makes SSL an increasingly popular paradigm in video analysis. SSL has recently yielded successful results in learning visual representations from unlabeled videos with various pretext tasks [9, 20, 45]. These methods use a backbone that has been pretrained with images or videos in a self-supervised manner to perform tasks on videos, including contrastive learning [19, 42, 45], self-distillation [9], or Masked Modeling which selects a random section of the input sequence to mask out, and then predicts the features of those sections [16, 20, 33, 40]. The learnt self-supervised model from the pretext task can be applied to any downstream computer vision tasks, including classification, segmentation, detection, etc.

**Motion in Action Recognition:** Motion cues[11, 24, 36] have been recognised as important for video understanding in the past few years. Most works use optical flow, a motion representation component in many video recognition techniques, to obtain the statistical motion labels required for their work [43], separating the background from the main objects in optical flow frames. In another work [23], a multi-task motion-guided video salient object detection network is proposed consisting of two sub-networks. One sub-network is used to detect salient objects in still images, and the other is used to detect motion saliency in optical flow images. Most motion descriptors use absolute motions and thus only work well when the camera and background are relatively static, such as Fleet & Jepson’s phase-based features [15] and Viola et al.’s generalised wavelet features [35]. Therefore, the critical problem is identifying characteristics that accurately capture the motion of hands or objects while impervious to the camera and backdrop motion.

## 3 Motion-focused Self-supervised Video Understanding

Fig. 2 overviews our method, with three parts; first, our automatic motion area detection; With optical flow input to create a motion map to remove camera motion. Second, we propose our new strategy for the SSL pretext task, a reconstruction task that focuses on masking 3D patches on the motion area in the video called MOFO (Motion Focused). Thirdly, the downstream task adaptation step emphasises motion further by integrating motion information during the training.

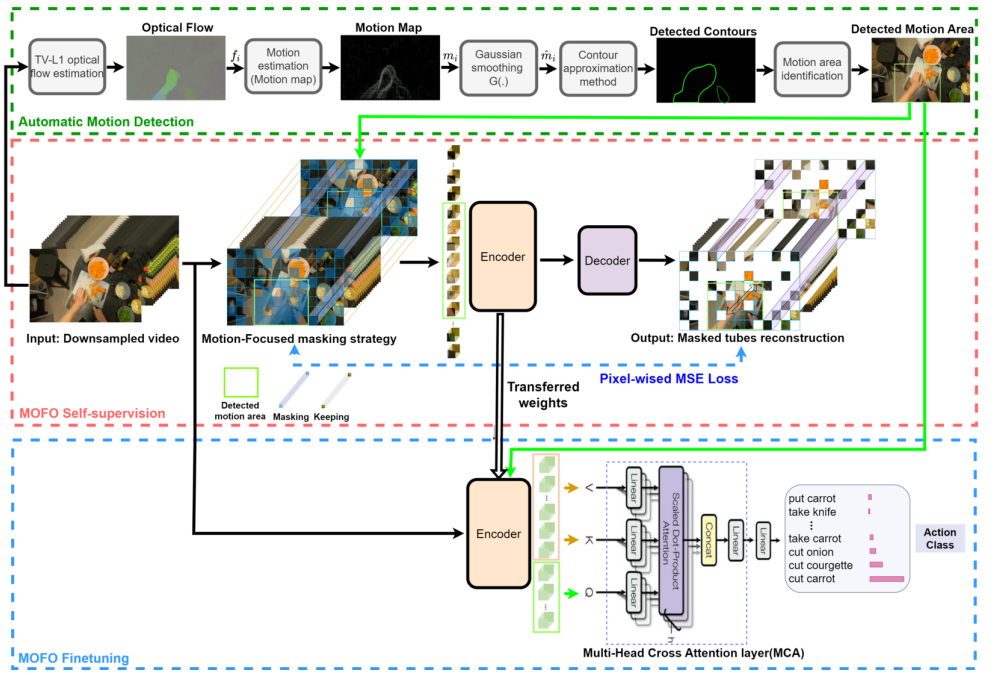


Figure 2: Our proposed MOFO self-supervision and finetuning frameworks.

### 3.1 Automatic Motion Area Detection

To identify the motion areas without pretrained object detectors, we propose using classical computer vision features, Optical flow vectors; however, these vectors will be affected by camera motion, with static objects or background pixels exhibiting high movement velocities in optical flow when the camera moves rapidly. To mitigate the problem above, we calculate the motion boundaries [6] and use these to define a motion map [24]. Therefore, given a video with  $T$  frames, and a  $H \times W$  dimension, we first extract the optical flow vectors representing  $\{f_i \in \mathbb{R}^{H \times W}\}_{i=1}^T$  pixel-level motion between two consecutive frames in a video using the TV-L1 algorithm [46] that offers increased robustness against illumination changes, occlusions and noise. Then given the horizontal and vertical displacements of each pixel between the  $i$ th frame and the  $(i+1)$ th frame represented by the flow maps  $u_i, v_i \in \mathbb{R}^{H \times W}$ , the resulting motion map is defined as:

$$m_i = \sqrt{\left(\frac{\partial u_i}{\partial x}\right)^2 + \left(\frac{\partial u_i}{\partial y}\right)^2 + \left(\frac{\partial v_i}{\partial x}\right)^2 + \left(\frac{\partial v_i}{\partial y}\right)^2} \quad (1)$$

where every component denotes the corresponding  $x$ - and  $y$ -derivative differential flow frames contributing towards computing  $m_i$ , representing moving velocity in the  $i$ -th frame while ignoring the camera motion. As a result,  $m_i \in \mathbb{R}^{H \times W}$  is less influenced by camera motion and considers the moving salients in the  $i$ -th frame. A low-pass Gaussian filter is used to smooth areas of the image with high-frequency components to reduce the unwanted noise effect further. The Gaussian Smoothing Operator computes an average of the surrounding pixels that are weighted according to the Gaussian distribution ( $G$ ), which is as follows:



$$G_{x,y} = \frac{1}{2\pi\sigma^2} \exp\left(-\frac{x^2+y^2}{2\sigma^2}\right) \quad (2)$$

$$\hat{m}_i = G * m_i$$

where  $\hat{m}$  is the convolved motion map by the Gaussian kernel.

To reduce unwanted noise, the values are filtered by their standard deviation and pixels with values less than 1.5 times the standard deviation are assigned a value of 0, keeping just the extremity pixels representing motion. After noise reduction, the next step is to find the boundaries of the motion. To do so, we create contours [31], which are short curves that connect points of the same hue or intensity. We select the two most significant contours in each frame to create a mask that indicates the motion area in a frame of a specific video. The main reason for choosing two contours is that in our datasets, an action is defined by hands and the corresponding object. We create a bounding box around the resulting area that precisely represents the motion in each video. In Fig. 5(a), we qualitatively compare our automatic box predictions and the provided supervised annotation for Epic-Kitchens-100 for several sample frames and provide further examples in the supplementary material.

## 3.2 Motion-focused Self-Supervised Learning

MOFO uses 3D tube volume embeddings for the self-supervised pretext stage to obtain 3D video patches from frames as inputs. It encodes these with a vanilla ViT [14] with joint space-time attention as a backbone. We segmented each video into  $N$  non-overlapping tubes  $\mathbf{p}_i \in \mathbb{R}^{H_i \times W_i \times T_i}$ . Then, we use a high-ratio tube masking approach to perform masked auto-encoder (MAE) pretraining with an asymmetric transformer-based encoder-decoder architecture reconstruction task. Unlike other often random masking methods, we explicitly integrate the motion information computed in Section 3.1 into our masking strategy resulting in a motion-guided approach to encode motion for our MAE. Our novel tube masking strategy enforces a mask to be allied on a high portion of the tubes inside the motion area. In other words, a fixed percentage of the tubes (generally 75%) inside the motion area is always randomly masked to ensure the model is attending more to the motion area at reconstruction time. A mean squared error (MSE) loss is computed in pixel space between the masked patches and trained reconstructed outputs. Our design encourages the network to capture more useful spatiotemporal structures, making MOFO a more meaningful task and improving the performance of self-supervised pretraining. All models only use the unlabelled data in the training set of each dataset for pretraining.

## 3.3 Motion-focused Finetuning

Recall that the self-supervised learning protocol is split between a pretraining and finetuning stage. We propose a new approach to focus on the motion area at both pretext and the finetuning of the model. To do so, we utilise the trained asymmetric transformer-based encoder-decoder architecture for the video self-supervised pretraining and replace the encoder.

For each video, the region with motion is identified, and a bounding box for this area of interest is generated without supervision in subsection 3.1. As the area inside the motion box has more semantic motion information, we wish to exploit this information for our task by leveraging the detected motion box. On the other hand, the video’s setting and any nearby

items could provide context for categorising the video clips for the action recognition task. For instance, in the case of washing dishes, the hands can be seen in the sink, but the dishes beside the sink may indicate that the person is washing them. To avoid missing motion area information and maintaining context from the outer area, we propose to use multi-cross attention (MCA) [22] in our encoder. MCA is an attention mechanism that mixes two different embedding sequences; the two are from the same modality. Unlike self-attention, where inputs are the same set, during cross-attention, they differ; MCA’s main objective is to determine attention scores using data from various information sources. This module resides between the encoder and MLP classifier layers, takes the inner and outer motion box embeddings, and outputs the fused embedding. This module aims to integrate the video context while concentrating on inner motion box embeddings by fusing outer and inner motion box embeddings. Given a set of patches  $\{\mathbf{p}_i\}_1^N$ , the transformer yields two sets of embeddings:  $\{\mathbf{e}^{\text{inner}}\}_{j=1}^{N_{\text{inner}}}$  for the inner motion boxes and  $\{\mathbf{e}^{\text{outer}}\}_{k=1}^{N_{\text{outer}}}$  for the outer ones, as described by:

$$\{\mathbf{e}^{\text{inner}}\}_{j=1}^{N_{\text{inner}}}, \{\mathbf{e}^{\text{outer}}\}_{k=1}^{N_{\text{outer}}} = \text{ViT}(\{\mathbf{p}_i\}_1^N) \quad (3)$$

These embeddings are then processed by a cross-attention mechanism, where  $Q$ ,  $K$ , and  $V$  represent query, key, and value, respectively. The CrossAttention function is formalised as follows:

$$\text{CrossAttention}(Q, K, V) = \text{softmax}\left(\frac{QK^T}{\sqrt{d_k}}\right)V \quad (4)$$

where  $Q = \mathbf{e}^{\text{inner}}$ ,  $K = V = \mathbf{e}^{\text{outer}}$ . In the context of multi-head attention, each attention head  $i$  is computed by applying the CrossAttention function to the query, key, and value matrices, each weighted by a different learned weight matrix  $W_i^Q \in \mathbb{R}^{d_{\text{model}} \times d_k}$ ,  $W_i^K \in \mathbb{R}^{d_{\text{model}} \times d_k}$ ,  $W_i^V \in \mathbb{R}^{d_{\text{model}} \times d_v}$  respectively:

$$\text{head}_i = \text{CrossAttention}(QW_i^Q, KW_i^K, VW_i^V) \quad (5)$$

Finally, the fused embedding  $\mathbf{e}^{\text{fused}}$  is computed by concatenating the results from all attention heads and then applying another learned weight matrix  $W^O \in \mathbb{R}^{hd_v \times d_{\text{model}}}$ . This multi-head cross-attention (MCA) operation can be represented as:

$$\mathbf{e}^{\text{fused}} = \text{MCA}(Q, K, V) = \text{Concat}(\text{head}_1, \dots, \text{head}_h)W^O \quad (6)$$

We employ  $h = 3$  parallel attention layers, or heads, in this work. We also use  $d_v = d_k = d_{\text{model}}$  for each. The model is ultimately finetuned with a cross-entropy loss  $\mathcal{L}$ :

$$\begin{aligned} \mathcal{L} &= - \sum_n \mathbf{y}_n \log \hat{\mathbf{y}}_n \\ \hat{\mathbf{y}} &= \text{FC}(\mathbf{e}^{\text{fused}}) \end{aligned} \quad (7)$$

where,  $\mathbf{y}_n$  is the true label for  $n$ th video clip,  $\hat{\mathbf{y}}_n$  is its predicted label, and FC is the fully connected layers typically used for classification.

## 4 Experiments

We conducted several experiments to assess the effectiveness of our proposed strategy. For self-supervised pretraining and to leverage the pretrained backbone on action recognition

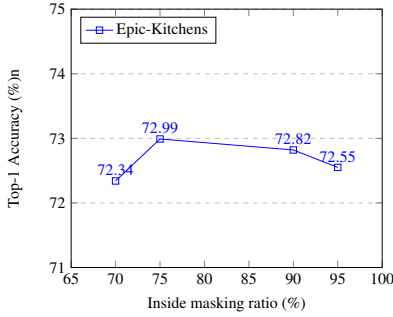


Figure 3: The effect of inside masking ratio on Epic-Kitchens-100 datasets demonstrates that a high inside masking ratio (75%) delivers the best efficiency and effectiveness trade-off.

downstream task, we use two well-known and large datasets to evaluate our proposed approach: **Epic-Kitchens-100** [14] and **Something-Something V2 (SSV2)** [18]. The former contains 97 verb classes, 300 noun classes and 3806 action classes which is a challenging egocentric dataset for action recognition from video data due to the background distractions and irrelevant objects. The latter is a large video dataset including 220,847 videos in the dataset, which focuses more on human-object interaction, with 174 classes.

## 4.1 Experimental Settings

MOFO uses ViT-Base as a decoder/encoder backbone, trained for 800 epochs on Something-Something V2 and Epic-Kitchens for the SSL independently. We follow the training and experiential parameters from recent work [63] to ensure a fair comparison and finetune for 100 epochs with early stopping. The model takes 16 frames from the video with  $224 \times 224$  size and divides the input video into a 3D  $16 \times 16 \times 8$  patch embeddings, resulting in  $H = 224$ ,  $W = 224$ ,  $T = 16$ ,  $H_t = 16$ ,  $W_t = 16$ ,  $T_t = 8$ , and  $N = 392$ . While we have a fixed number of input patches for our model, we do not have a fixed number of inner  $N_{\text{inner}}$  and outer  $N_{\text{outer}}$  embeddings due to varying size of the motion area in each video clip. We report Top-1 accuracy on Epic-Kitchens and Top-1 and Top-5 accuracy on Something-Something on downstream tasks and use Pytorch and DeepSpeed [21] on 4xNVIDIA Quadro RTX-5000 GPU for our experiments.

## 4.2 Results and analysis

The recognition accuracy for our MOFO SSL using regular finetuning is reported in Table 1 shown as MOFO\*. We demonstrate significant performance improvement over the other self-supervised approaches, comparable to the best-supervised approach. Our strategy outperforms approaches like OmniMAE [16], trained jointly on images and videos by 3.2% in Top-1 accuracy. On Something Something V2 our method outperforms VIMPAC [62] and ST-MAE [14], which both use ViT-Large as a backbone, whereas our backbone is vanilla ViT-Base with over 3x fewer parameters. Compared to VideoMAE [63], our approach achieves significantly better results while the number of backbone parameters remains the same. While MOFO\*\* indicates our result with pretraining on non-motion SSL and MOFO fine-tuning, which further increases accuracy, MOFO<sup>†</sup> denotes the MOFO SSL and MOFO fine-tuning, and this provides the greatest performance, by increasing 2.6%, 2.1%, 1.3%

Table 1: Human activity recognition on **Epic-Kitchens** and **SomethingSomething** in terms of Top-1 and Top-5 accuracy. **blue: This is the result computed by us using the public code** MOFO\* is pretrained by our MOFO SSL and used non-motion finetuning. MOFO\*\* This is our result with pretraining on non-motion SSL and has MOFO finetuning. MOFO<sup>†</sup> denotes the MOFO SSL and MOFO finetuning.

Method	Backbone	Param	SomethingSomething		Epic-Kitchens		
			Action		Verb	Noun	Action
			Top-1	Top-5	Top-1	Top-1	Top-1
Supervised							
TDN <sub>EN</sub> [57]	ResNet101x2	88	69.6	92.2	-	-	-
SlowFast [18]	ResNet101	53	63.1	87.6	65.6	50.0	38.5
TSM [25]	ResNet-50	-	63.4	88.5	67.9	49.0	38.3
MViTv1 [16]	MViTv1-B	37	67.7	90.9		-	-
TimeSformer [8]	ViT-B	121	59.9	-	-	-	-
TimeSformer [8]	ViT-L	430	62.4	-	-	-	-
ViViT FE [8]	ViT-L	-	65.9	89.9	66.4	56.8	44.0
Mformer [28]	ViT-B	109	66.5	90.1	66.7	56.5	43.1
Mformer [28]	ViT-L	382	68.1	91.2	67.1	57.6	44.1
Video SWin [26]	Swin-B	88	69.6	92.7	67.8	57.0	46.1
Self-supervised							
VIMPAC [82]	ViT-L	307	68.1	-	-	-	-
BEVT [83]	Swin-B	88	70.6	-	-	-	-
VideoMAE [63]	ViT-B	87	70.8	92.4	71.6	66.0	53.2
ST-MAE [14]	ViT-L	304	72.1	-	-	-	-
OmnMAE [16]	ViT-B	87	69.5	-	-	-	39.3
Omnivore(Swin-B) [14]	ViT-B	-	71.4	93.5	69.5	61.7	49.9
Ours(MOFO*)	ViT-B	87	72.7	94.2	73.0	67.1	54.1
Ours(MOFO**)	ViT-B	102	74.7	95.0	74.0	68.0	54.5
Ours(MOFO <sup>†</sup> )	ViT-B	102	75.5	95.3	74.2	68.1	54.5

accuracy over the best-performing methods on Epic-Kitchens verb, noun and action classification and 4.7% on Something Something V2 action classification respectively.

**Visualizing self-supervised representation** To further understand the representations learnt by MOFO, we utilize GradCAM [80] to create a saliency map highlighting each pixel’s importance to show how each pixel contributes to the discrimination of the video clip. Fig. 4 visualizes the middle frame of a video clip, the motion map of the VideoMAE and our MOFO from the fifth attention layer of the ViT-Base backbone. It is interesting to note that for similar actions: *knead dough*, *cut carrot*, and *cut-in tomato*, MOFO is sensitive to the location that is the most significant motion location as detected by our automatic algorithm. Additionally, in Fig. 4’s middle row, the MOFO model not only detects the motion area but also highlighted the direction of the hand movement. The representations learned by MOFO align the motion map more effectively than those learned by VideoMAE. Additionally, the regions of high importance in these representations serve as solid visual evidence for describing the video clip. As a result, the representations learned by MOFO may be more robust. These findings further demonstrate the effectiveness of utilizing motion in MOFO for SSL.

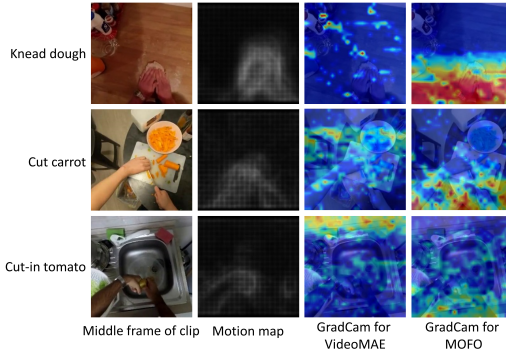


Figure 4: From left to right: video clip middle frame, motion map, Grad-CAM attention map for VideoMAE, Grad-CAM attention map for MOFO

### 4.3 Ablation studies

We evaluate the contribution of the different components of our approach.

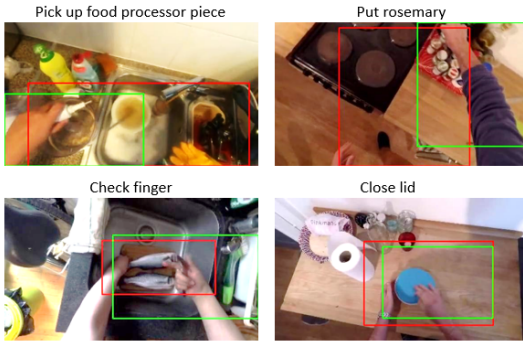
**Masking ratio.** VideoMAE [83] recommended tube masking with an extremely high ratio which helps reduce information leakage during masked modelling. They demonstrated the best efficiency and efficacy with a masking ratio of 90%. Therefore we explore the effect of the inside masking ratio for verb classification on Epic-Kitchens in Fig. 3. It shows that the model pretrained with a masking ratio of 90% as the general masking ratio for a video and a high ratio for inside masking ratio (75%) achieves the highest efficiency level. Thus, we continue experimenting with the rest by fixing the inside mask ratio to 75%.

**Automatic vs. supervised motion area detection.** We compare the results using our automatically detected-motion areas and the ground truth bounding box annotation provided by [2] on the Epic-Kitchens dataset in Table 5(b). Our automatic motion detection results are close compared to supervised annotations, as seen in Table 5(b), despite the challenging camera motion from the egocentric videos.

We compute the Intersection over Union (IoU) metric to compare our automatic detector with the supervised annotated bounding boxes on both datasets. For the Epic-Kitchens dataset, the IoU is 40%, and for Something-Something V2 the IoU is 31%. Although these numbers are lower, our automatic motion detection only detects motion and ignores unnecessary static objects near the motion. As you can see in Fig. 5(a), our automatic motion box still focuses on the motion area and object of interest, which is the key requirement.

## 5 Conclusions

MOFO introduces a Motion-Focused technique, which explores the motion information for enhancing motion-aware self-supervised video action recognition. More specifically, we represent the video exclusively through patches of the inside of the motion area that contain information about the outside of the motion area. Extensive experiments on two challenging datasets demonstrate that this context-based SSL technique improves performance in action recognition tasks, and the public code will guide many research directions.



(a)

Figure 5: (a) Comparison between the unsupervised and supervised motion area detection, green rectangles indicate the unsupervised while red ones show supervised detected motion area. (b) Effect of supervised vs. automatic motion area utilisation in MOFO.

Method	Annotation	<b>Epic-Kitchens</b>
		Verb Top-1
MOFO supervision	Supervised	73.26
	Automatic(ours)	72.99

(b)

## References

- [1] Arif Akar, Ufuk Umut Senturk, and Nazli Ikizler-Cinbis. MAC: mask-augmentation for motion-aware video representation learning. In *BMVC*, 2022.
- [2] Anurag Arnab, Mostafa Dehghani, Georg Heigold, Chen Sun, Mario Lučić, and Cordelia Schmid. Vivit: A video vision transformer. In *ICCV*, 2021.
- [3] Gedas Bertasius, Heng Wang, and Lorenzo Torresani. Is space-time attention all you need for video understanding? In *ICML*, 2021.
- [4] Mathilde Caron, Hugo Touvron, Ishan Misra, Hervé Jégou, Julien Mairal, Piotr Bojanowski, and Armand Joulin. Emerging properties in self-supervised vision transformers. In *ICCV*, 2021.
- [5] Ting Chen, Simon Kornblith, Kevin Swersky, Mohammad Norouzi, and Geoffrey E. Hinton. Big self-supervised models are strong semi-supervised learners. In *NeurIPS*, 2020.
- [6] Navneet Dalal, Bill Triggs, and Cordelia Schmid. Human detection using oriented histograms of flow and appearance. In *ECCV*, 2006.
- [7] Dima Damen, Hazel Doughty, Giovanni Maria Farinella, Antonino Furnari, Evangelos Kazakos, Jian Ma, Davide Moltisanti, Jonathan Munro, Toby Perrett, Will Price, et al. Rescaling egocentric vision: Collection, pipeline and challenges for epic-kitchens-100. *IJCV*, 2022.
- [8] Jacob Devlin, Ming-Wei Chang, Kenton Lee, and Kristina Toutanova. BERT: pre-training of deep bidirectional transformers for language understanding. In *NAACL*, pages 4171–4186, 2019.
- [9] Carl Doersch, Abhinav Gupta, and Alexei A Efros. Unsupervised visual representation learning by context prediction. In *ICCV*, pages 1422–1430, 2015.

- [10] Alexey Dosovitskiy, Lucas Beyer, Alexander Kolesnikov, Dirk Weissenborn, Xiaohua Zhai, Thomas Unterthiner, Mostafa Dehghani, Matthias Minderer, Georg Heigold, Sylvain Gelly, et al. An image is worth 16x16 words: Transformers for image recognition at scale. *arXiv preprint arXiv:2010.11929*, 2020.
- [11] Victor Escorcia, Ricardo Guerrero, Xiatian Zhu, and Brais Martinez. Sos! self-supervised learning over sets of handled objects in egocentric action recognition. In *ECCV*, 2022.
- [12] Haoqi Fan, Bo Xiong, Karttikeya Mangalam, Yanghao Li, Zhicheng Yan, Jitendra Malik, and Christoph Feichtenhofer. Multiscale vision transformers. In *ICCV*, 2021.
- [13] Christoph Feichtenhofer, Haoqi Fan, Jitendra Malik, and Kaiming He. Slowfast networks for video recognition. In *ICCV*, 2019.
- [14] Christoph Feichtenhofer, haoqi fan, Yanghao Li, and Kaiming He. Masked autoencoders as spatiotemporal learners. In *Advances in Neural Information Processing Systems*. Curran Associates, Inc., 2022.
- [15] David J. Fleet and Allan D. Jepson. Stability of phase information. *IEEE TPAMI*, 1993.
- [16] Rohit Girdhar, Alaaeldin El-Nouby, Mannat Singh, Kalyan Vasudev Alwala, Armand Joulin, and Ishan Misra. Omnimae: Single model masked pretraining on images and videos. *arXiv preprint arXiv:2206.08356*, 2022.
- [17] Rohit Girdhar, Mannat Singh, Nikhila Ravi, Laurens van der Maaten, Armand Joulin, and Ishan Misra. Omnivore: A single model for many visual modalities. In *CVPR*, 2022.
- [18] Raghav Goyal, Samira Ebrahimi Kahou, Vincent Michalski, Joanna Materzynska, Susanne Westphal, Heuna Kim, Valentin Haenel, Ingo Fruend, Peter Yianilos, Moritz Mueller-Freitag, et al. The "something something" video database for learning and evaluating visual common sense. In *ICCV*, 2017.
- [19] Sheng Guo, Zihua Xiong, Yujie Zhong, Limin Wang, Xiaobo Guo, Bing Han, and Weilin Huang. Cross-architecture self-supervised video representation learning. In *CVPR*, 2022.
- [20] Agrim Gupta, Stephen Tian, Yunzhi Zhang, Jiajun Wu, Roberto Martín-Martín, and Li Fei-Fei. Maskvit: Masked visual pre-training for video prediction. *arXiv preprint arXiv:2206.11894*, 2022.
- [21] Conglong Li, Zhewei Yao, Xiaoxia Wu, Minjia Zhang, and Yuxiong He. Deepspeed data efficiency: Improving deep learning model quality and training efficiency via efficient data sampling and routing. *arXiv preprint arXiv:2212.03597*, 2022.
- [22] Dong Li, Ting Yao, Zhaofan Qiu, Houqiang Li, and Tao Mei. Long short-term relation networks for video action detection. In *ACM International Conference on Multimedia*, 2019.
- [23] Haofeng Li, Guanqi Chen, Guanbin Li, and Yizhou Yu. Motion guided attention for video salient object detection. In *ICCV*, 2019.



- [24] Rui Li, Yiheng Zhang, Zhaofan Qiu, Ting Yao, Dong Liu, and Tao Mei. Motion-focused contrastive learning of video representations. In *ICCV*, 2021.
- [25] Ji Lin, Chuang Gan, and Song Han. Tsm: Temporal shift module for efficient video understanding. In *ICCV*, 2019.
- [26] Ze Liu, Jia Ning, Yue Cao, Yixuan Wei, Zheng Zhang, Stephen Lin, and Han Hu. Video swin transformer. In *CVPR*, June 2022.
- [27] Arsha Nagrani, Shan Yang, Anurag Arnab, Aren Jansen, Cordelia Schmid, and Chen Sun. Attention bottlenecks for multimodal fusion. *NeurIPS*, 2021.
- [28] Mandela Patrick, Dylan Campbell, Yuki Asano, Ishan Misra, Florian Metze, Christoph Feichtenhofer, Andrea Vedaldi, and João F Henriques. Keeping your eye on the ball: Trajectory attention in video transformers. *Advances in neural information processing systems*, 2021.
- [29] Zhaofan Qiu, Ting Yao, Chong-Wah Ngo, Xinmei Tian, and Tao Mei. Learning spatio-temporal representation with local and global diffusion. In *CVPR*, 2019.
- [30] Ramprasaath R Selvaraju, Michael Cogswell, Abhishek Das, Ramakrishna Vedantam, Devi Parikh, and Dhruv Batra. Grad-cam: Visual explanations from deep networks via gradient-based localization. In *ICCV*, 2017.
- [31] Satoshi Suzuki et al. Topological structural analysis of digitized binary images by border following. *Computer vision, graphics, and image processing*, 1985.
- [32] Hao Tan, Jie Lei, Thomas Wolf, and Mohit Bansal. Vimpac: Video pre-training via masked token prediction and contrastive learning. *arXiv preprint arXiv:2106.11250*, 2021.
- [33] Zhan Tong, Yibing Song, Jue Wang, and Limin Wang. Videomae: Masked autoencoders are data-efficient learners for self-supervised video pre-training. *NeurIPS*, 2022.
- [34] Du Tran, Lubomir Bourdev, Rob Fergus, Lorenzo Torresani, and Manohar Paluri. Learning spatiotemporal features with 3d convolutional networks. In *ICCV*, 2015.
- [35] Paul Viola, Michael J Jones, and Daniel Snow. Detecting pedestrians using patterns of motion and appearance. *IJCV*, 2005.
- [36] Jiangliu Wang, Jianbo Jiao, Linchao Bao, Shengfeng He, Yunhui Liu, and Wei Liu. Self-supervised spatio-temporal representation learning for videos by predicting motion and appearance statistics. In *CVPR*, 2019.
- [37] Limin Wang, Zhan Tong, Bin Ji, and Gangshan Wu. Tdn: Temporal difference networks for efficient action recognition. In *CVPR*, 2021.
- [38] Rui Wang, Dongdong Chen, Zuxuan Wu, Yinpeng Chen, Xiyang Dai, Mengchen Liu, Yu-Gang Jiang, Luowei Zhou, and Lu Yuan. Bevt: Bert pretraining of video transformers. In *CVPR*, 2022.
- [39] Xiaolong Wang and Abhinav Gupta. Videos as space-time region graphs. In *ECCV*, 2018.

- [40] Chen Wei, Haoqi Fan, Saining Xie, Chao-Yuan Wu, Alan Yuille, and Christoph Feichtenhofer. Masked feature prediction for self-supervised visual pre-training. In *CVPR*, 2022.
- [41] Qizhe Xie, Minh-Thang Luong, Eduard Hovy, and Quoc V Le. Self-training with noisy student improves imagenet classification. In *CVPR*, 2020.
- [42] Ceyuan Yang, Yinghao Xu, Jianping Shi, Bo Dai, and Bolei Zhou. Temporal pyramid network for action recognition. In *CVPR*, 2020.
- [43] Charig Yang, Hala Lamdouar, Erika Lu, Andrew Zisserman, and Weidi Xie. Self-supervised video object segmentation by motion grouping. In *ICCV*, 2021.
- [44] Xitong Yang, Xiaodong Yang, Sifei Liu, Deqing Sun, Larry Davis, and Jan Kautz. Hierarchical contrastive motion learning for video action recognition. *arXiv preprint arXiv:2007.10321*, 2020.
- [45] Sukmin Yun, Hankook Lee, Jaehyung Kim, and Jinwoo Shin. Patch-level representation learning for self-supervised vision transformers. In *CVPR*, 2022.
- [46] Christopher Zach, Thomas Pock, and Horst Bischof. A duality based approach for realtime tv-l 1 optical flow. In *Pattern Recognition*, 2007.

## Supplementary Materials

In this supplementary material, we provide more details on our MOFO model:

- In Section 6, we visualized the reconstructed samples comparing our MOFO model with VideoMAE [83] on both SomethingSomething V2 [88] and Epic-Kitchen [9] datasets.
- In Section 7, we explore how MOFO finetuning behaves and visualize GradCAM using MOFO self-supervision in 7.2. In subsection 7.1, we investigate the effect of the number of depths and heads in MCA.
- In the last Section 8, we provide more samples showing how our automatic motion area detection performs.

## 6 Motion-focused Self-Supervised Learning

This section shows several reconstructed image frames from a video in Fig. 6 and Fig. 7. In order to accomplish video self-supervised pre-training tube masking with a high ratio for MAE pre-training, we use an asymmetric encoder-decoder architecture. We can reconstruct the masked patches by finding the spatially and temporally corresponding unmasked patches in the adjacent frames while using random tube masking. The mean squared error (MSE) loss between normalised masked tokens and reconstructed tokens in pixel space serves as the loss function. Videos are all randomly chosen from the validation sets of both datasets. Our proposed MOFO model ensures that a fixed number of masks exist within the motion area compared to the VideoMAE model. These examples suggest that, compared to VideoMAE, our MOFO model reconstructs the samples in the motion area significantly more accurately,

demonstrating that the model has focused its attention on the motion area. We can produce satisfying reconstruction results, especially in the area where motion occurs with our MOFO by applying extremely high ratio masking at random (90%) while always masking a fixed percentage of the tubes (75%) inside the motion area.

## 7 Motion-focused Finetuning

We explore the MOFO finetuning in the following subsections.

### 7.1 MCA Hyper-parameters Ablation

We list the MCA hyperparameters used in our MOFO finetuning experiments here. We experiment with various head and depth settings when Epic-Kitchens is the target dataset shown in Table 7.1. We experiment with these parameters for the verb task on Epic-Kitchens in order to find the best choice for our cross-attention layer that we suggested for MOFO finetuning. The final head and depth are 3 and 1 respectively.

Table 2: Ablation experiment for number of head and depth in MOFO finetuning

Finetuning method	Backbone training	CA heads	CA depths	<b>Epic-Kitchens</b>
				Verb Top-1
VideoMAE	VideoMAE	-	-	71.6
MOFO	VideoMAE	1	1	73.5
MOFO	VideoMAE	1	2	73.8
MOFO	VideoMAE	1	3	73.6
MOFO	VideoMAE	2	1	73.7
MOFO	VideoMAE	2	2	73.3
MOFO	VideoMAE	<b>3</b>	<b>1</b>	<b>74.0</b>
MOFO	VideoMAE	3	2	73.5
MOFO	VideoMAE	4	1	73.8
MOFO	VideoMAE	4	2	73.3

### 7.2 Visualization of GradCAM using MOFO self-supervision

We visualize the GradCAM and motion map in Fig. 8 for the samples in which VideoMAE can't identify the class but our MOFO can. The attention maps show how effective our approach is in capturing the motion area.

## 8 Automatic Motion Area Detection

In Fig. 9, we present additional qualitative examples of our automatic motion area detection compared with the provided supervised annotation for Epic-Kitchens and SomethingSomething V2 datasets. These samples show that our proposed automatic motion area detection minimises the impact of the static object in the motion box while highlighting the motion areas. Our automatic motion box concentrates on the area and item of interest, which is a crucial necessity for our proposed approach, even for self-supervision or finetuning.

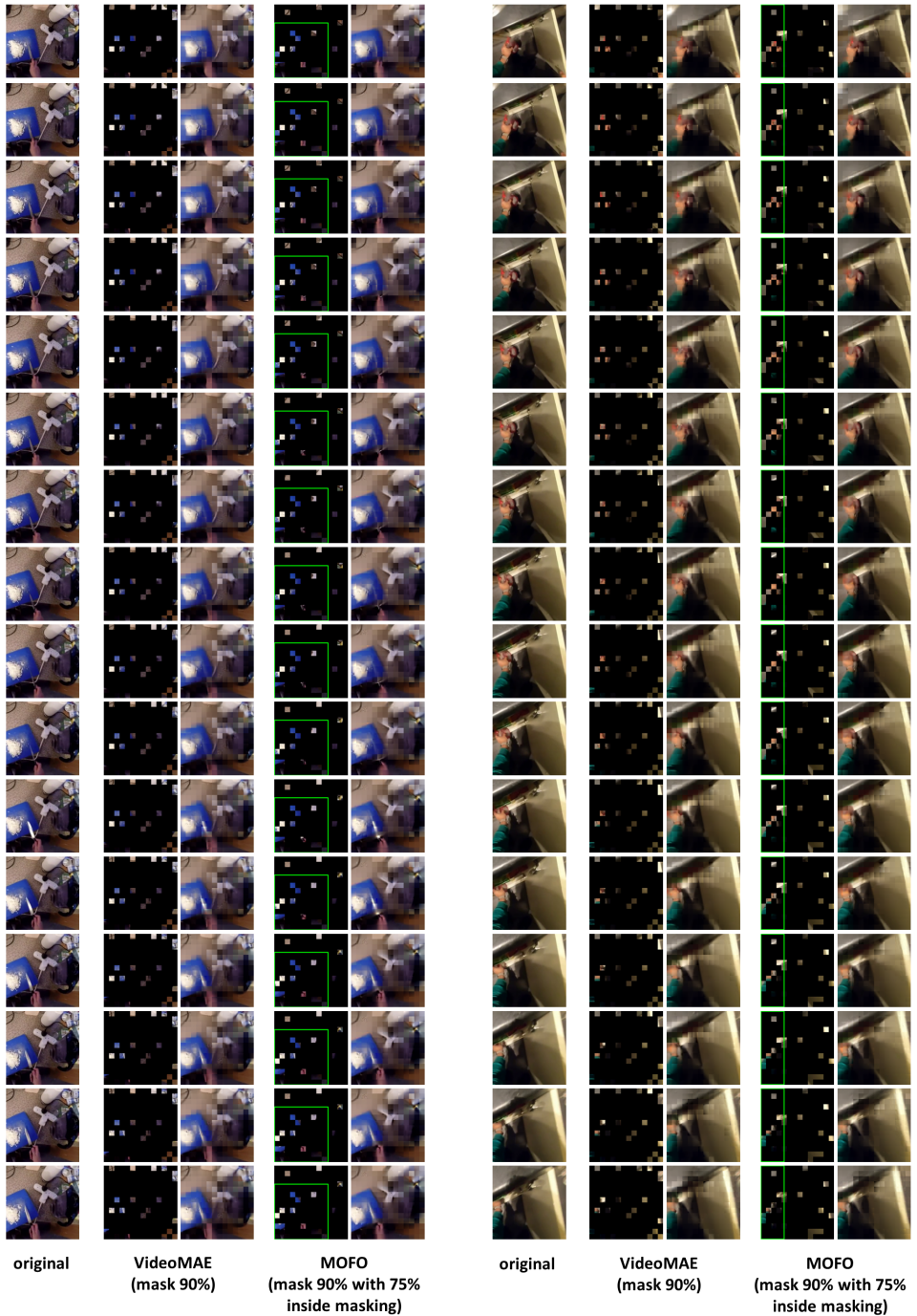
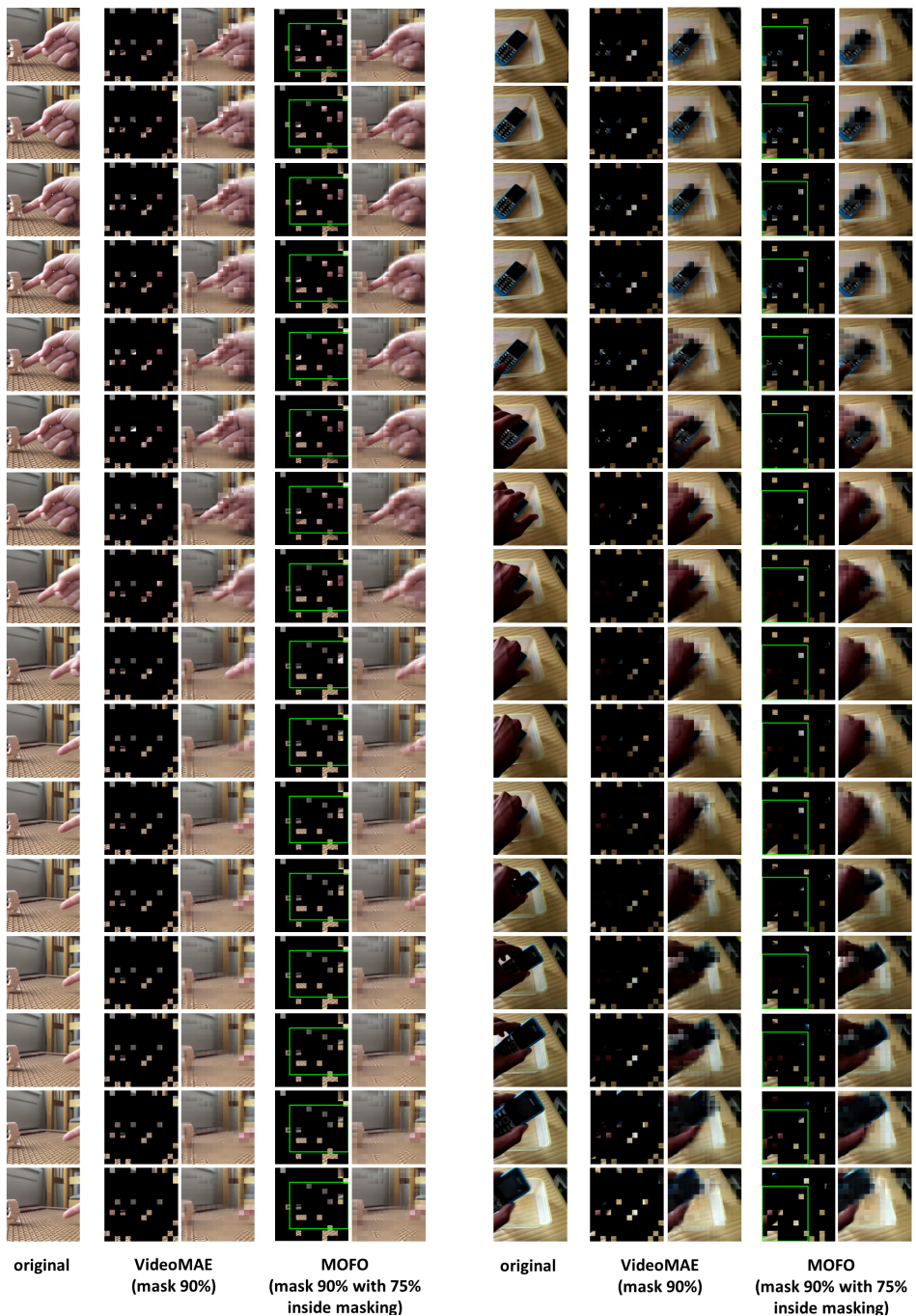


Figure 6: Qualitative Comparison on reconstructions using VideoMAE and MOFO on **Epic-Kitchens** dataset. MOFO Reconstructions of videos are predicted by MOFO pre-trained with a masking ratio of 90% and an inside masking ratio of 75% .





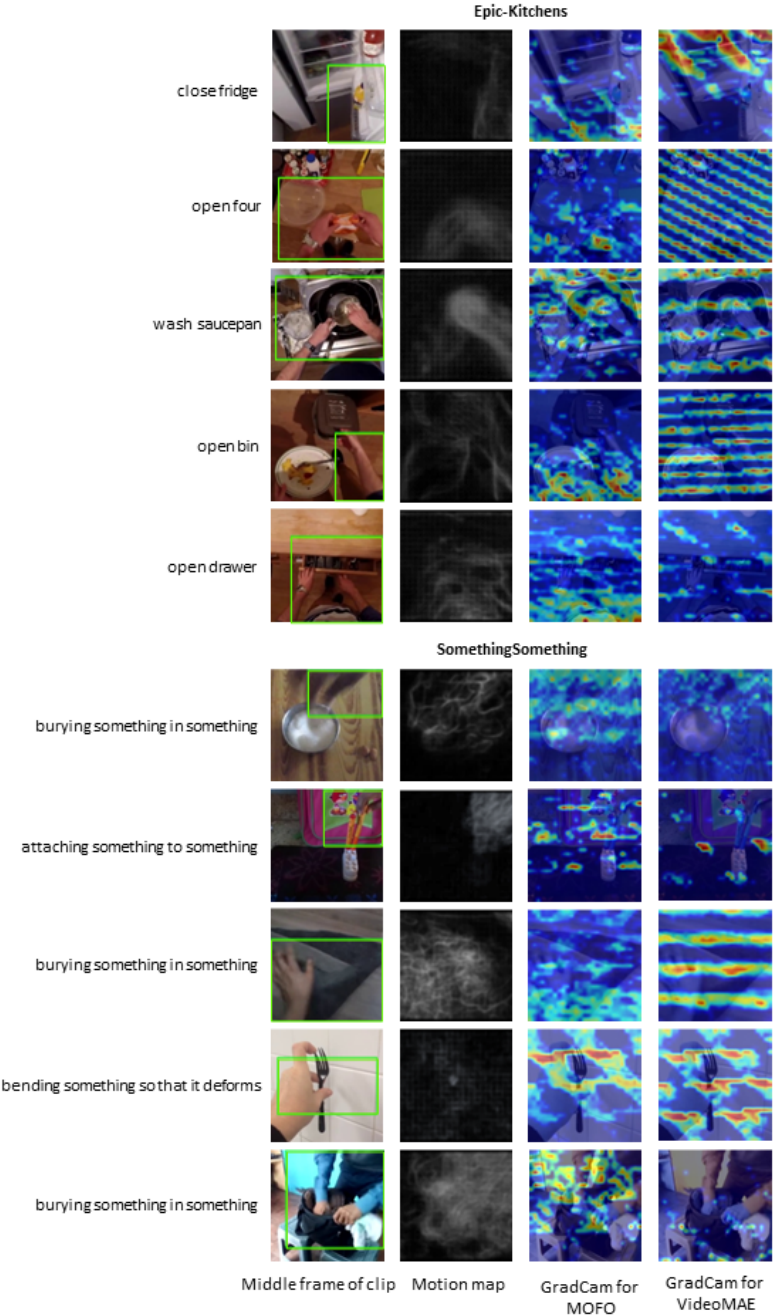


Figure 8: We visualize the attention maps generated by GradCAM based on VideoMAE and MOFO for Epic-Kitchens and SomethingSomething V2 dataset. The attention maps show that our proposed approach can better capture the motion area.

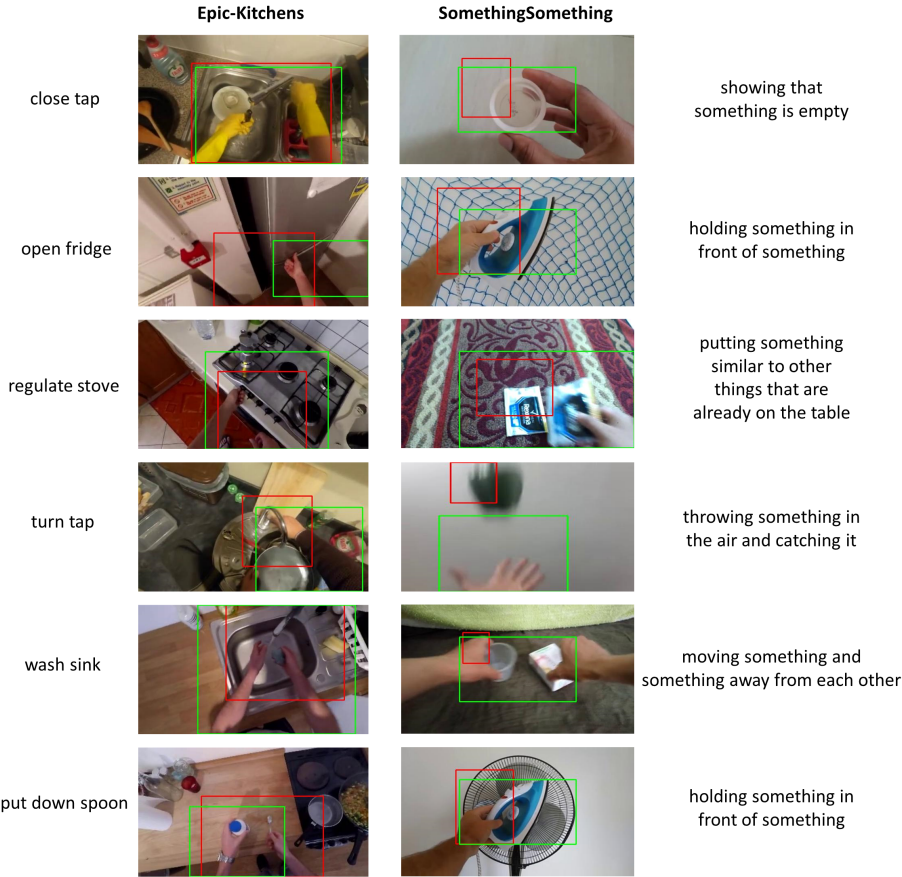


Figure 9: Comparison between the unsupervised and supervised motion area detection, green rectangles indicate the unsupervised while red ones show supervised detected motion area.